magnetochemistry

MDPI

Article

Phase Transformation of Kaolin-Ground Granulated Blast Furnace Slag from Geopolymerization to Sintering Process

Noorina Hidayu Jamil [1,2,*], Mohd. Mustafa Al Bakri Abdullah [1], Faizul Che Pa [1], Mohamad Hasmaliza [3], Wan Mohd Arif W. Ibrahim [1], Ikmal Hakem A. Aziz [1], Bartłomiej Jeż [4,*] and Marcin Nabiałek [4]

[1] Center of Excellence Geopolymer and Green Technology, Universiti Malaysia Perlis, Kangar 01000, Perlis, Malaysia; mustafa_albakri@unimap.edu.my (M.M.A.B.A.); faizul@unimap.edu.my (F.C.P.); wmarif@unimap.edu.my (W.M.A.W.I.); ikmalhakem@unimap.edu.my (I.H.A.A.)
[2] Faculty of Mechanical Engineering Technology, Universiti Malaysia Perlis, Kangar 01000, Perlis, Malaysia
[3] Biomaterial Research Niche Group, School of Materials and Mineral Resources Engineering, Universiti Sains Malaysia, Nibong Tebal 14300, Penang, Malaysia; hasmaliza@usm.my
[4] Department of Physics, Częstochowa University of Technology, Al. Armii Krajowej 19, 42-200 Częstochowa, Poland; nmarcell@wp.pl
* Correspondence: noorinahidayu@unimap.edu.my (N.H.J.); bartek199.91@o2.pl (B.J.)

Abstract: The main objective of this research was to investigate the influence of curing temperature on the phase transformation, mechanical properties, and microstructure of the as-cured and sintered kaolin-ground granulated blast furnace slag (GGBS) geopolymer. The curing temperature was varied, giving four different conditions; namely: Room temperature, 40, 60, and 80 °C. The kaolin-GGBS geopolymer was prepared, with a mixture of NaOH (8 M) and sodium silicate. The samples were cured for 14 days and sintered afterwards using the same sintering profile for all of the samples. The sintered kaolin-GGBS geopolymer that underwent the curing process at the temperature of 60 °C featured the highest strength value: 8.90 MPa, and a densified microstructure, compared with the other samples. The contribution of the Na_2O in the geopolymerization process was as a self-fluxing agent for the production of the geopolymer ceramic at low temperatures.

Keywords: kaolin; GGBS; sintering geopolymer; self-fluxing

Citation: Jamil, N.H.; Abdullah, M..M.A.B.; Che Pa, F.; Hasmaliza, M.; W. Ibrahim, W.M.A.; A. Aziz, I.H.; Jeż, B.; Nabiałek, M. Phase Transformation of Kaolin-Ground Granulated Blast Furnace Slag from Geopolymerization to Sintering Process. *Magnetochemistry* **2021**, *7*, 32. https://doi.org/10.3390/magnetochemistry7030032

Academic Editors: Sabina Lesz and Mats Johnsson

Received: 20 December 2020
Accepted: 19 February 2021
Published: 26 February 2021

1. Introduction

Kaolin is widely used as a source of aluminosilicate in geopolymer. However, the direct use of kaolin in geopolymer i.e., without preliminary treatment, such as thermal, mechanical or chemical treatment may yield a slower rate of aluminium (Al) dissolution. Furthermore, sufficient time has to be allowed for interactions among the component materials [1,2]. Parameters, such as the sodium hydroxide concentration and curing regime, are important factors that must be taken into consideration when designing a kaolin-based geopolymer product for a specific application [1]. The liquid content consists of sodium silicate (Na_2SiO_3) and sodium hydroxide (NaOH). Sodium silicate acts as an alkali activator, binder, plasticiser or dispersant. In contrast, sodium hydroxide with a high pH will assist the dissolution reaction of the aluminosilicate sources which is followed by precipitation [3,4].

Ground granulated blast furnace slag (GGBS) is one of the most used waste materials in the production of geopolymer materials. The primary component in GGBS, i.e., CaO, has been reported to be an effective component for the development of high compressive strength in a geopolymer. The addition of CaO to the composition improves the hardening process [5]. The optimum temperature and duration of curing are essential in the geopolymerization reaction, in order to achieve high strength. During the curing process, the geopolymer mortar and concrete undergo a polymerisation reaction.

Previous research has described the use of room temperature, or slightly elevated temperatures in the range between 60 and 80 °C, for the synthesis of phosphate-based

geopolymers [6]. Elevated temperatures have been shown to yield phosphate-based geopolymers with improved mechanical properties (29.9 MPa), compared with those obtained at room temperature (20.7 MPa). A previous study showed that the sintered kaolin geopolymer was prepared by the powder pressing method and sintered until 1250 °C. The maximum flexural strength of 86 MPa was achieved at 1200 °C using a 12 M kaolin geopolymer. However, sintering at 1250 °C leads to melting of the geopolymer body [7].

The phase development after sintering is dependent on several parameters, including the mineralogical phase composition of the raw materials, used for the preparation of the ceramic mixtures, and the temperature at which the ceramic structure is sintered or fired [4]. Conventional approaches for sintering glass-ceramics usually include two steps: Vitrification of raw materials at high temperatures (1300 to 1500 °C), followed by nucleation and crystal growth [8]. However, a study on the compressive strength of palm oil fuel ash and fly ash based geopolymer mortars had used two-steps of the sintering profile and it shows that the result obtained was also influenced by the source of aluminosilicate material [9].

Investigation properties of kaolin geopolymer, following sintering, has not gained much interest due to the limitation of the low reactivity properties of kaolin during geopolymerization. The purpose for sintering the geopolymer was to study the capability of using raw kaolin as a geopolymer precursor with the addition of GGBS in phase transformation. This explains the current research interest in investigating the effect of curing temperature, in the range from room temperature up to 80 °C, on the sintered kaolin-GGBS geopolymer. The following factors are considered: Strength properties, evolution of microstructure, and phase transformation.

2. Materials and Methods

The investigated geopolymer samples were made from kaolin, and GGBS was mixed with an alkali activator using a mechanical stirrer until a slurry with a solid to liquid ratio of 2:1 was produced. The homogenised mixture was poured into a mould. The alkali activator was prepared 24 h prior to use, by mixing sodium hydroxide (NaOH) with sodium silicate at Na_2SiO_3 to NaOH ratio of 4:1. The NaOH flakes were purchased from Formosa Plastic Corporation, Taiwan with a purity of 99%. The liquid sodium silicate was purchased from the South Pacific Chemical Industries Sdn. Bhd., Malaysia with chemical composition of 30.1% SiO_2, 9.4% Na_2O and 60.5% H_2O (SiO_2/Na_2O ratio of 3.20). The geopolymer slurry was vibrated, to remove trapped air, and sealed with plastic at the exposed portion of the mould during the curing stage. The samples were allowed to cure at room temperature for 24 h.

Next, the curing process was continued, using different curing temperatures. There were four selected temperatures, namely: Room temperature (RT), 40, 60, and 80 °C, for 14 days. The samples were demoulded afterwards. The samples were divided into two sets, "as-cured" and "sintered". The as-cured samples were sintered using a heating profile, as shown in Figure 1. Step 1 was sintered at a lower temperature (T1): 500 °C with a heating rate of 2 °C/min. A higher temperature (T2) was applied in step 2: 900 °C with a heating rate of 4 °C/min. The "soaking" time was set to 1 h for each step. The cooling rate was 10 °C/min. The kaolin-GGBS geopolymer was sintered using a bench-top muffle furnace. The purpose of using two-steps of the sintering process in this work was to reduce the major cracking, since the as-cured kaolin-GGBS geopolymer was directly sintered without the powder pressing method.

The phase composition of the raw materials and kaolin-GGBS geopolymer were determined using X-ray diffraction (XRD). A Bruker D8 Advance XRD, USA equipped with a copper anode (Cu Ka, λ 1.5406 Å), was used for this process. Prior to this analysis, dry-powder samples were compacted. Analysis results were recorded within a 2θ range of 5–80°, using a scanning rate of 0.1 deg/s, and the data were analysed using the X'Pert HighScore Plus software. The semi-quantitative analysis calculates the estimated mass

fractions of the accepted phases. The scale factor and reference intensity ratio (RIR) values from the database are used to perform the calculation. A semi-quantitative result is automatically calculated when all the required data are available. The result is shown in the pattern list. Semi-quantitative results are only calculated if RIR values and scale factors for all the accepted phases are available. Meaningful semi-quantitative results are achieved, when the accepted phases represent 100% of the phases of the sample, where all the phases must be identified.

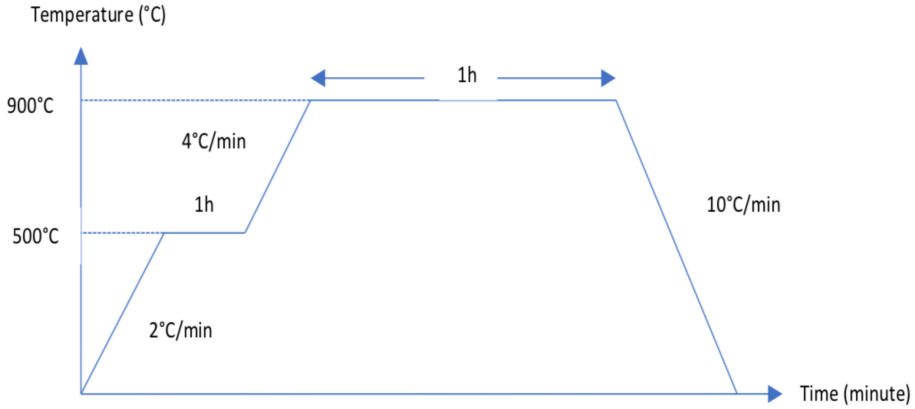

Figure 1. Two-step sintering profile for sintering the kaolin-ground granulated blast furnace slag (GGBS) geopolymer.

Fourier transform infrared spectroscopy (FTIR) was performed, using a Perkin Elmer Spectrum One, USA, to characterise the structural surfaces of the raw materials and the sintered kaolin-GGBS geopolymer within the range of 400–1400 cm^{-1}. Using an agate mortar, the potassium bromide (KBr) powder was mixed with a glass powder in a ratio of 9:1. The powder mixture was compressed, using a hand-press machine, into the form of transparent pellets each with a diameter of <5 mm. The microstructure was imaged by a Zeiss Supra 35VP scanning electron microscope (SEM) using an accelerating voltage of 5 kV. The specimens were divided into small pieces and surface-ground in order to obtain a flat surface. The samples were placed under a vacuum for 1 h and coated with Au-Pd on their main surfaces, for imaging purposes.

3. Results and Discussion

3.1. Raw Materials Characterisation

The diffraction patterns obtained from raw kaolin and ground granulated blast furnace slag are shown in Figure 2. Kaolin consists of kaolinite ($Al_4(OH)_8(Si_4O_{10})$), silicon oxide SiO_2, and fibroferrite ($Fe(OH)(SO_4)(H_2O)_5$) in crystalline phases. According to the semi-quantitative analysis, the kaolin used in this study is composed of: ~88% kaolinite, ~7% silicon oxide, and ~5% fibroferrite. Ground granulated blast furnace slag contains proportions of both an amorphous glassy phase and a crystalline phase. Therefore, it can be considered to be a semi-crystalline phase. The crystalline phase consists of Calcite ($CaCO_3$, ~35%), Akermanite ($Ca_2Mg(Si_2O_7)$, ~32%), and Quartz (SiO_2, ~34%). However, the phase quantification of the semi-quantitative analysis was only for crystalline phases.

The FTIR spectrum of kaolin and GGBS was divided into three regions as shown in Figure 3. The absorption bands within 3620 to 3696 cm^{-1} was being observed in the first region of kaolin indicating the ordered structure of kaolinite. However, the hydroxyl intensities at this region did not occur in GGBS to its disordered structure, as per the XRD results. The main functional groups of kaolin are Si-O and Al-OH at the third region between 1300 to 450 cm^{-1}. The intensity of ~1451 cm^{-1} in GGBS second region was due to the asymmetric stretching of the CO_3^{2-} ion, indicating traces of carbonates. Davidovits (2013) characterized this band as the CO_3 stretching vibration mode caused by

the presence of calcite due to the reaction between excess calcium oxide and atmospheric carbon dioxide [10].

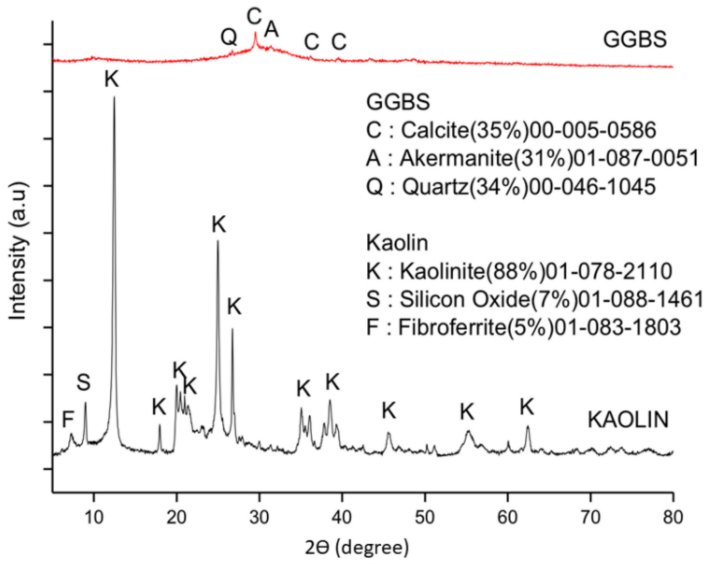

Figure 2. Quantitative analysis of phase composition of kaolin and GGBS.

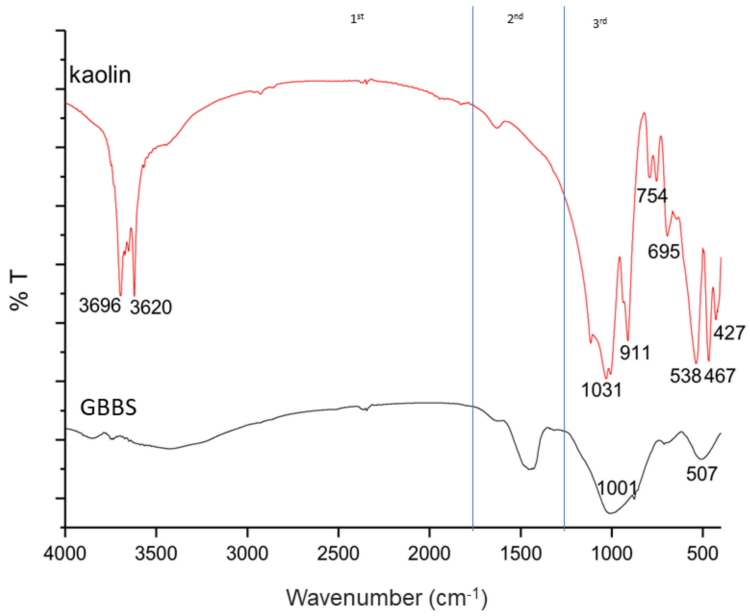

Figure 3. Fourier transform infrared spectroscopy (FTIR) spectrum of kaolin and GGBS.

Figure 4 shows a layered microstructure of kaolin in (**a**) and granulate-shape of GGBS in (**b**). The probable thickness of the kaolin plates existed in ~100 nm based on the scale in the micrograph. Meanwhile, GGBS have a large surface with deposition of spherical particles. The shape of GGBS was influenced by the milling process processing [11].

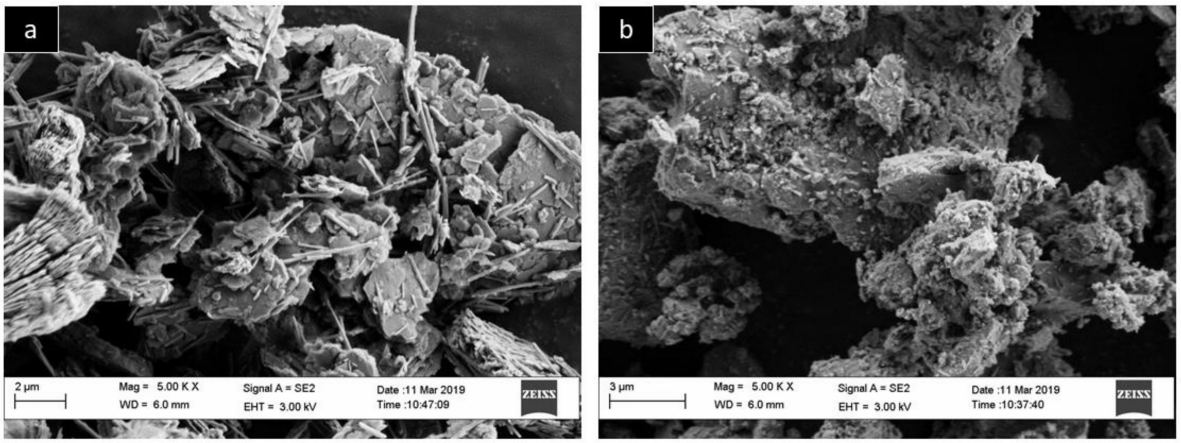

Figure 4. Microstructure of (**a**) kaolin and (**b**) ground granulated blast furnace slag.

3.2. Phase Composition of As-Cured and Sintered Kaolin-GGBS Geopolymer

Figure 5 presents the results of XRD analyses of the kaolin-GGBS geopolymer "after curing for 14 days at four different temperatures", compared with "after sintering at up to 900 °C". There were significant differences in the phase compositions between "after curing" and "after sintering". The crystalline phase of kaolinite and the silicon oxide phase from kaolin were still remaining in all of the kaolin-GGBS geopolymer samples after curing at all temperatures. The quartz phase of GGBS was observed in the as-cured samples. The Albite $Na(AlSi_3O_8)$ phase occurred at the higher curing temperatures, i.e., 60 and 80 °C. This phase was transformed drastically after sintering, as shown in all of the samples of the sintered kaolin-GGBS geopolymer. The phase composition percentages in the as-cured and sintered kaolin-GGBS geopolymer samples are presented in Tables 1 and 2, respectively.

Table 1. Phase composition of the as-cured kaolin-GGBS geopolymer (%).

Curing Temperature (°C)	RT	40	60	80
K: Kaolinite ($Al_4(OH)_8(Si_4O_{10})$)	77	77	63	67
S: Silicon Oxide (SiO_2) $(SiO_2)_{64}$	5	5	5	4
Q: Quartz (SiO_2) SiO_2	18	18	14	2
AL: Albite (heat-treated) $Na(AlSi_3O_8)$	-	-	20	27

Table 2. Phase composition of the sintered kaolin-GGBS geopolymer (%).

Curing Temperature (°C)	RT	40	60	80
Q: Quartz (SiO_2)	20	2	14	22
AL: Albite (heat treated) $Na(AlSi_3O_8)$	32	74	43	48
A: Akermanite ($Ca_2Mg(Si_2O_7)$ $Ca_2Mg(Si_2O_7)$	10	10	7	12
N: Nepheline (Si-rich) $Na_7(Al_6Si_{10}O_{32})$	38	13	36	-
M: Magnetite (Fe_3O_4) Fe_3O_4	-	-	-	6
D: Diopside-ferrian, $(Ca(MgFe_{0.5})(Si2Fe_{0.5})O_6)$	-	-	-	38

The occurrence of kaolinite phase in the as-cured samples in the range of 63% to 77% indicates incomplete geopolymerization. It shows that some of the silicon and aluminium in the kaolin is mainly in the crystal form. Due to the high crystallinity of kaolin itself, the dissolution process was prolonged and only occurred on the surface particles of the kaolin. It was believed that the strength is related to the dissolution of ions in the kaolin. It was

estimated that the slow reactivity of kaolin provided insufficient dissolved ions for further reorganisation and polycondensation reactions to form hydrated products. In addition to kaolinite, the crystallinity of the silicon oxide (SiO_2) phase in kaolin was remaining in all the as-cured samples, making up ~5% of the composition.

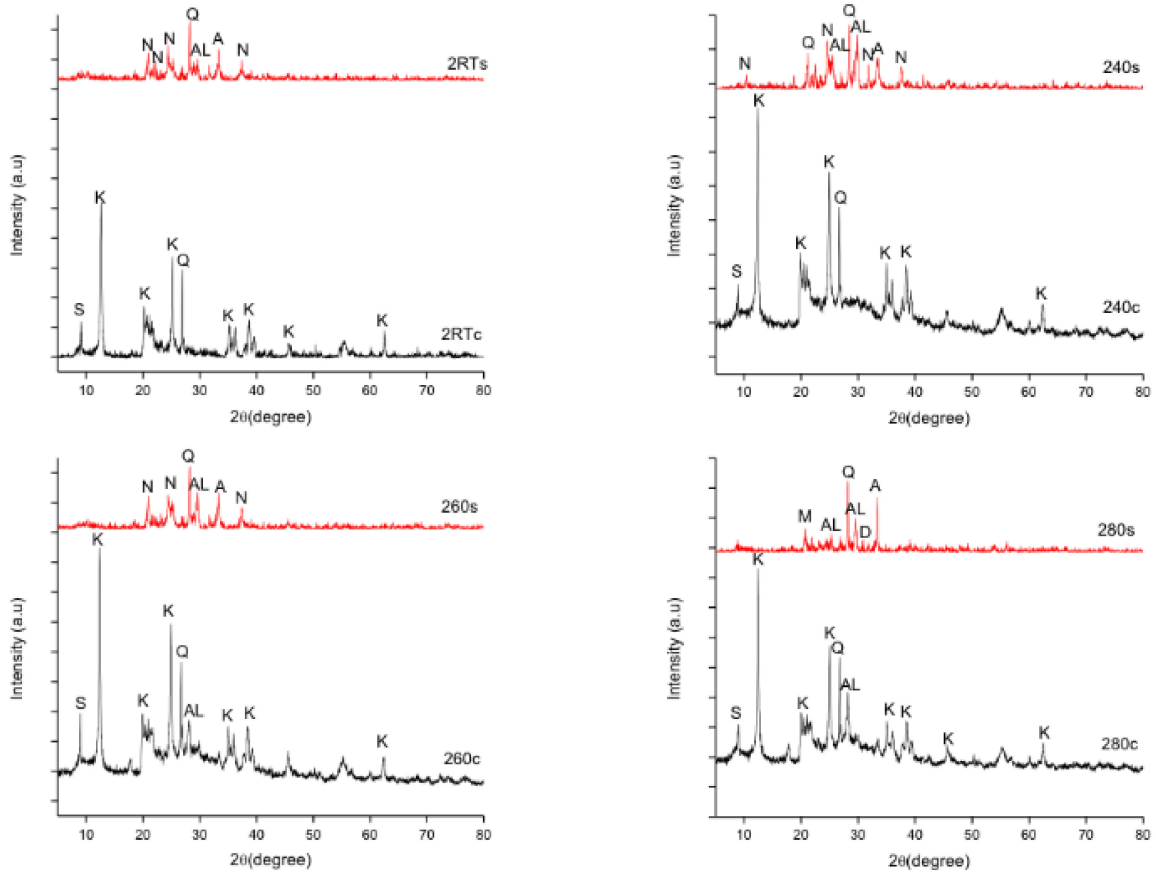

Figure 5. Phase composition of the as-cured and sintered kaolin-GGBS geopolymer.

The degree of crystallinity of quartz (SiO_2) from GGBS at 20 to 28° had increased after 14 days of curing, indicating the reaction between kaolin and GGBS during geopolymerization. The addition of GGBS, with its disordered structure, had accelerated the combination reactions, leading to the formation of the geopolymer. When kaolinite is heated, the adsorbed water is liberated at above 100 °C, and the weakest part of the chemical bond is broken. Then, dehydroxylation takes place at 450–600 °C. For kaolinite, dehydroxylation might result in the disturbance of the $Al(O,OH)_6$ octahedral sheet by the outer hydroxyl groups, but does not have much effect on the SiO_4 tetrahedral sheet due to the more stable inner hydroxyl groups.

The outer hydroxyls of the octahedral sheets may be more easily removed by heating than the inner ones which will maintain a more ordered SiO_4 tetrahedral group within the structure during dehydroxylation. After heating at 950 °C, the SiO_4 groups combine with AlO_6 groups to form the Al-Si spinel phase in a short-range order structure. Therefore, kaolinite phases disappeared after sintering. According to Mierzwiński et al. (2019), after sintering of the geopolymer, the peaks for kaolinite should disappear while the peak for quartz remains [12].

The loss of kaolinite and silicon oxide intensity after sintering suggests the formation of the nepheline phase. This phase transformation occurs through the release of chemically bonded hydroxyl groups of kaolinite. It is noted that the compressive strength values of samples cured at 60 °C have approximately half of the strength of the sintered kaolin-GGBS

geopolymer. The presence of nepheline in the sintered samples leads to an increase in the compressive strength. The increase in strength was less pronounced at 80 °C, after sintering, due to the disappearance of nepheline and the appearance of magnetite and diopside-ferrian. Both magnetite and diopside-ferrian phases contain the element Fe, which was contributed from the fibroferrite phase in kaolin.

The formation of magnetite (Fe_3O_4) and diopside-ferrian, $Ca(MgFe_{0.5})(Si_2Fe_{0.5})O_6$, occurred after sintering, in samples cured at 80 °C. The formation of this iron-based phase was contributed from the fibroferrite phase in the raw kaolin. According to Chen and Tuan (2001), the reaction of Fe_2O_3 to Fe_3O_4 can take place, liberating the O_2 gas, as the temperature reaches ~1500 °C [13]. Therefore, the so-called "bloating" is due to the release of O_2 gas from the reaction of Fe_2O_3 to Fe_3O_4. As a result, the microstructure of these sintered materials featured large pores with an interconnected pattern. This was also indicated physically by a decrease in the compressive strength. However, this phenomenon occurs at a lower temperature during sintering at 900 °C, due to the self-fluxing reaction during the geopolymerization process.

Albite phases occurred in samples after curing at 60 and 80 °C. This transformation is due to the presence of a high alkalinity solution (NaOH, 8 M), which activates the compound crystalline structure and leads to a straightforward chemical reaction between different oxides to form new phases. According to Mierzwiński et al. (2019), in the synthesis of geopolymers, the final properties are influenced by both the amorphous metakaolin phase and the residual kaolin content [7]. Higher phases of kaolin content adversely affect the mechanical strength of the geopolymer.

The formation of albite and nepheline after sintering was influenced by a reaction between the kaolinite and the alkali activator, as elaborated in Equation (1). However, the equations are not precisely balanced for many ceramic products and are more or less non-stoichiometric. Furthermore, the various oxides in the starting powder can induce a liquid phase during firing. The presence of the liquid phase can shift slightly the formation temperature of each phase and its amount. Albite and nepheline consist of the same elements, namely: Na, Al, Si, and O. During geopolymerization, the function of Na cations was to balance the negative charges created by the formation of Si-O-Al bonding, or by non-bridging oxygen ions remaining in the system. Meanwhile, OH^- was consumed during the hydrolysis of kaolin.

The Na_2O content was contributed by the Na_2SiO_3 and NaOH solutions. Sintering leads to a transformation of the crystalline phase, especially kaolinite, into an amorphous reactive one. Therefore, most of the gained strength arises from the GGBS, in addition to the enhancement effect of the NaO from the alkali activator. The densified area in the sintered kaolin-GGBS geopolymer was contributed by Na_2O, which was in accordance with the research by Lao et al. (2020), regarding the influences of Na_2O impurities in kaolin that had promoted microstructure densification of a ceramic at a relatively low temperature of less than 1200 °C [14].

$$\underset{\text{(Crystalline kaolinite)}}{Al_4(OH)_8(Si_4O_{10})} + \underset{\text{(Alkali activator)}}{Na_2SiO_3 + NaOH} \xrightarrow[\text{Sintering}]{} \underset{\text{(Nepheline)}}{Na_7(Al_6Si_{10}O_{32})} + \underset{\text{(Albite)}}{Na(AlSi_3O_8)} \quad (1)$$

$$\underset{\text{(Amorphous akermanite)}}{Ca_2Mg(Si_2O_7)} \xrightarrow[\text{Sintering}]{} \underset{\text{(Crystalline akermanite)}}{Ca_2Mg(Si_2O_7)} \quad (2)$$

Akermanite existed in an amorphous phase in GGBS. After sintering, the degree of crystallinity of akermanite was increased in all the sintered kaolin-GGBS geopolymers with the composition range from 7% to 12% as simplified in Equation (2). Heat-curing is necessary to achieve a geopolymer with good strength properties. This could be attributed to the higher strength obtained after sintering, compared with the as-cured samples. The amorphous minerals of the mix led to the consolidation of texture which improves the compressive strength of the geopolymer. Generally, akermanite belongs to the melilite group, which possesses good wear resistance and corrosion resistance.

3.3. Structural Spectra Analysis

The Fourier-transform infrared (FTIR) spectra collected on the as-cured and sintered kaolin-GGBS geopolymer samples are shown in Figure 6. The presence of water in the geopolymers is evidenced by the high-frequency bands at 3600 and 1646 cm^{-1}, related to the O-H stretching and bending modes of molecular water, as shown in the first region, respectively. Both bands indicate the kaolinite phase from kaolin. The presence of OH groups is linked to the structure, and also water molecules, which are adsorbed onto the surface or entrapped in the large cavities of the geopolymer framework. However, the intensity of 3600 cm^{-1} is broad, compared with the same peak in kaolin, which indicates a considerable disorder of hydroxyl groups and water molecules. The reduction of peak intensity suggests the transformation of crystalline kaolinite to an amorphous phase during geopolymerization.

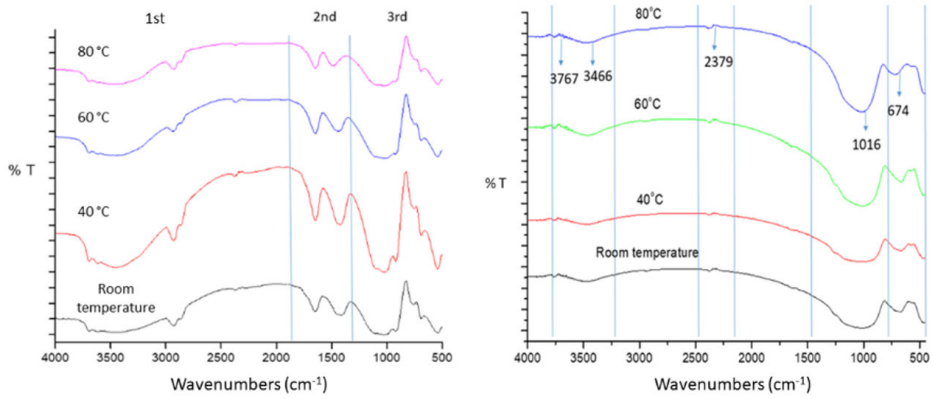

Figure 6. FTIR spectrum of the (**a**) as-cured kaolin-GGBS geopolymer and (**b**) sintered kaolin-GGBS geopolymer.

The spectra collected on the cured geopolymer samples display, in the second region, peaks at frequencies around 1400 cm^{-1}. A peak in this region is characteristic of the presence of the stretching vibration of CO_2. This is related to the decomposition of $CaCO_3$ in the GGBS, releasing CO_2. The magnitude of the calcite phase in the XRD pattern of GGBS was reduced after curing. The decomposition of calcite is described in Equation (3).

$$CaCO_3 \rightarrow CaO + CO_2 \quad (3)$$

The third region was considered as a significant fingerprint for the aluminosilicate geopolymer. Generally, the peaks are becoming broad and smooth between wavenumbers of 450 and 900 cm^{-1}, compared to kaolin. The difference in magnitude was the same as for the phase of kaolinite obtained in the XRD results. The band at 467 cm^{-1} indicates the bending vibration of Si-O-Si and O-Si-O occurring in the kaolin and as-cured samples.

A strong peak at ~1016 cm^{-1} in all the sintered samples is associated with Al-O and Si-O asymmetric stretching vibrations, characteristic of geopolymerization, and the presence of an amorphous aluminosilicate network structure. A broad peak in the region 3400 to 3600 cm^{-1} was due to the stretching vibrations of OH groups from the water molecules. The amorphous nature of the geopolymer is influenced by the type of alkali cation. The FTIR analysis confirms that dehydroxylation of the kaolin after sintering causes the total removal of a hydroxyl group. This demonstrates that the dehydroxylation causes a structural modification of the kaolinite present in kaolin.

Curing at a higher temperature does seem to influence the development of compressive strength in a positive way. However, when the geopolymer was subjected to the sintering process, 60 °C was found to be the optimum curing temperature resulting in the highest strength. It is interesting to note, that curing at a higher temperature (80 °C)

appears to weaken the compressive strength after sintering the geopolymer. It is believed that the sintering mechanism broke-down the structure of the geopolymer, resulting in dehydration and massively interconnected pores.

3.4. Compressive Strength

Figure 7 shows the compressive strength values for the cured and sintered kaolin-GGBS geopolymer samples, which were cured at four different curing temperatures. Generally, the compressive strength was found to increase when the specimens were cured from room temperature to 80 °C, and after sintering. However, a reduction was noticed in the 80 °C sintered kaolin-GGBS geopolymer. This shows that heat-curing accelerates the early strength development of materials. According to Dariusz et al., curing at highly elevated temperatures (39.85 to 41.85 °C) for a prolonged period causes deterioration of the sample due to the destabilisation of the silicate-Si-O-Al-O bond [12]. However, it depends on the sources of materials used to produce the geopolymer.

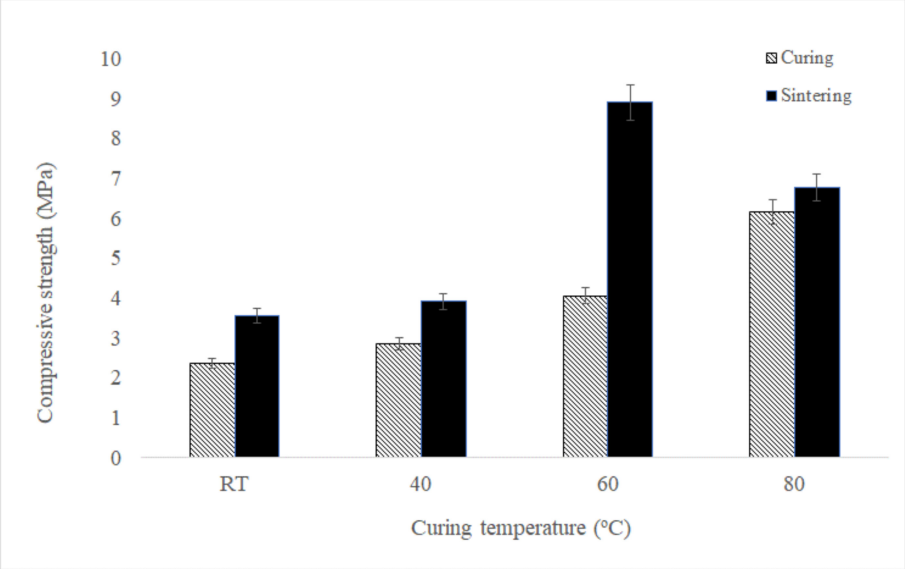

Figure 7. Effect of curing temperature on the compressive strength of cured and sintered kaolin-GGBS geopolymer samples.

The compressive strength trend for as-cured samples indicates the influence of high temperature in obtaining the early strength development of materials. The lowest compressive strength obtained was 2.35 MPa when curing at room temperature. The strength increased slightly, to 2.84 MPa, when the samples were cured at 40 °C. There were no significant effects on strength due to a slight increment of the curing temperature, away from room temperature (~27 °C) to 40 °C. The strength increased gradually to 4.04 and 6.16 MPa at 40 and 60 °C, respectively. The curing temperature played essential roles in both the acceleration of chemical reactions and the determination of the extent of the reaction during geopolymerization.

The highest resulting strength was observed at 60 °C, with 8.90 MPa after sintering, it was reduced at 80 °C. However, very high curing temperatures may destabilise the hardener and hinder proper geopolymerization. This shows that curing at a higher temperature had distorted the reaction and led to the failure of the sintered kaolin-GGBS geopolymer.

The cubic shape of the kaolin-GGBS geopolymer sample was physically stable, without major cracking observed after sintering, as shown in Figure 8. Each sample was differentiated by its curing temperature, namely: Room temperature, 40, 60, and 80 °C. There was no evident damage, such as the absence of edges and corners, in any of the sintered samples. However, there were crack initiations in sintered kaolin-GGBS geopolymer samples for

room temperature and 40 °C. Higher curing temperatures (i.e., 60 and 80 °C) resulted in more stability with less crack initiation after sintering.

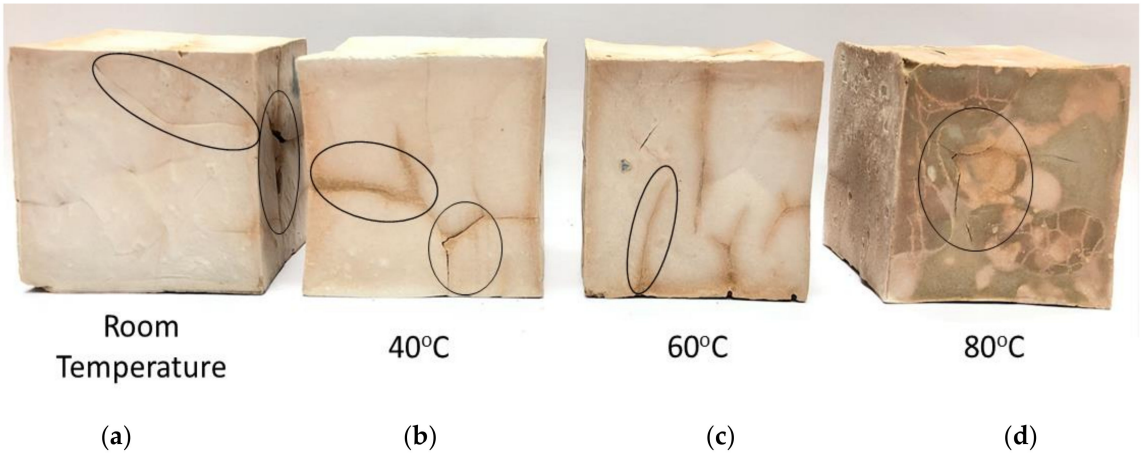

Figure 8. Visual appearance of kaolin-GGBS geopolymer samples with different curing temperatures. (**a**) Room temperature, (**b**) 40, (**c**) 60, and (**d**) 80 °C.

This indicates that the phenomenon of crack initiation was reduced when the curing temperature was increased. This is due to the quantity of excess water that did not evaporate completely during curing. One of the factors, exerting a strong influence on the process of crack initiation and propagation within the sintered geopolymer, is the presence of pores in the structure. It is reasonable to assume that the effect of pores varies depending on the curing temperature, water evaporation, and chemical composition in the kaolin-GGBS geopolymer.

3.5. Microstructure Characterisation

Images of the microstructure of the samples, taken after curing for 14 days and sintering at 900 °C, are shown in Figure 9. There were needle-shaped formations in the microstructure of as-cured kaolin-GGBS geopolymer samples of: Room temperature, 40 and 60 °C. However, the needle-shaped formations were not found in the microstructure of the 80 °C sample following curing. The effect of sintering can be seen from the changes of microstructure in (b) after sintering at 900 °C. Generally, the kaolin-GGBS geopolymer was densified after sintering, along with the formation of pores.

As seen in Figure 9a, an interlocking structure of flake-like kaolin appeared in the microstructure of samples after 14 days of curing. Wei et al. (2017) reported that the flake-like morphology was attributed to the substitution of Mg^{2+} by Al^{3+} in the octahedral positions of the kaolin structure [15]. The contribution of Mg^{2+} was from the akermanite phase in GGBS. This proves the reaction that occurred between kaolin and GGBS, with an alkali activator, during geopolymerization although the kaolin had not undergone heat treatment.

The formation of needle-shaped particles was more pronounced in samples cured at 60 °C, compared with samples cured at lower temperatures. The needle-shaped particles represent a small particle size, as observed at 60 °C, indicating that a smaller particle size leads to a larger surface area and a finer grade of porosity between the particles, as shown in Figure 10. The larger surface area contributed to the high reactivity of geopolymerization indicated by the high compression strength obtained after sintering. The morphology of "needles" and "broken flakes" represent the randomly ordered crystals of kaolinite due to dehydroxylation. The disordered structure represents the huge reactive potential during geopolymerization. The formation of pores was also observed at 80 °C after curing.

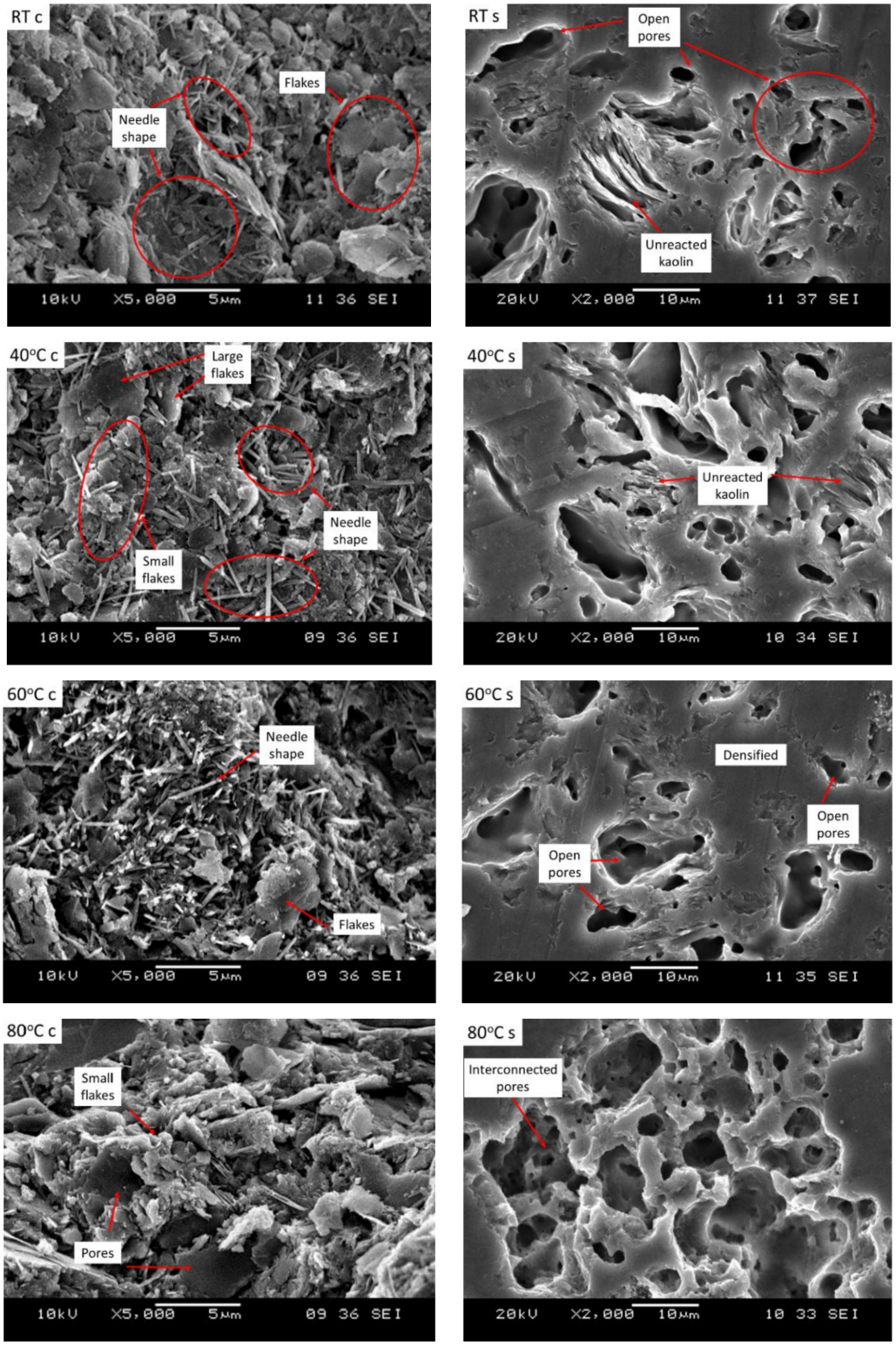

(**a**) As-cured kaolin-GGBS geopolymer. (**b**) Sintered kaolin-GGBS geopolymer.

Figure 9. Microstructure of as-cured (**a**) and sintered (**b**) kaolin-GGBS geopolymer samples, at different curing temperatures.

The formation of pores occurred in all samples of the sintered kaolin-GGBS geopolymer, as shown in Figure 9b. The unreacted kaolin is characterised by a layered structure, similar to that in the raw micrographs, and this was observed in the sintered kaolin-GGBS

geopolymer, RT, and 40 °C after sintering. The microstructure with an optimum densification area was observed at the curing temperature of 60 °C. This is due to the dissolving polymeric materials at the first stage (500 °C) of sintering. The formation of open pores was also found in this micrograph. This microstructure was interrelated with the high compressive strength obtained at this temperature. Pore pressure effects represent one of the critical factors that affect the strength evolution of sintered geopolymer at a high temperature. The higher pressure will accelerate water evaporation and create massive pores, thus leading to the low strength of the samples.

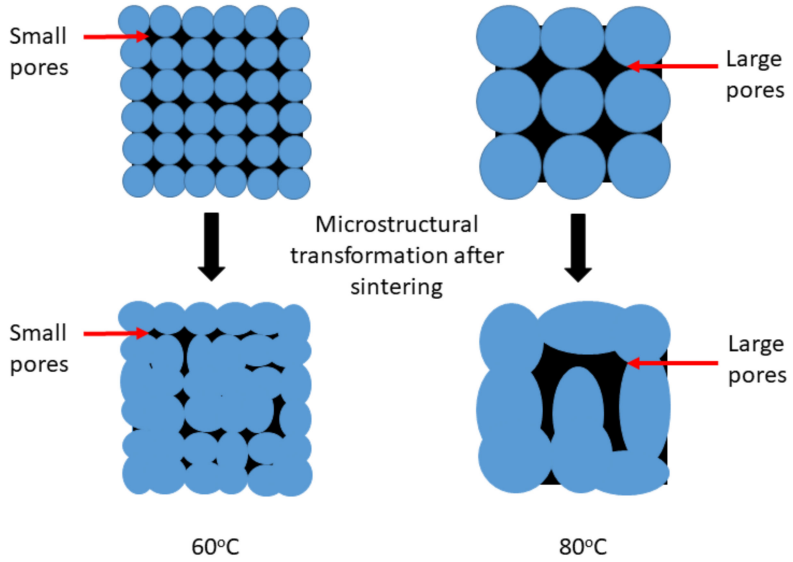

Figure 10. Schematic image of the pores in larger and smaller particle sizes and the transformation after sintering, based on the SEM images of kaolin-GGBS geopolymer at 60 and 80 °C.

In the 80 °C sample after sintering, geopolymerization was not well established due to the short-range period of geopolymerization indicated by the rapid water loss. This can be proved by the absence of needle-shape formations being observed in the microstructure of the 80 °C after the curing sample. However, the existence of CaO leads to the early strength development. The presence of calcite leads to the reinforcement of the mechanical strength of the geopolymer [16]. The reshaping of the pores after sintering is due to the kaolin and GGBS reactions. This led to the formation of micropores with an interconnected formation during sintering. This was observed as a pronounced feature in Figure 9b at 80 °C after sintering and indicated a reduction in compressive strength.

4. Conclusions

Despite the fact that similar phases were found, with comparable peak magnitudes in all of the cured and sintered samples, the compressive strength values were different in these samples. Thus, the development of compressive strength was linked with the reaction during geopolymerization. The crystalline kaolinite phase remained in the as-cured samples at four different curing temperatures. Kaolinite reacted with the alkali activator during sintering and stimulus phase transformation to nepheline and other phases. Curing at 60 °C resulted in the highest compressive strength with a densified microstructure. The sintering of the kaolin-GGBS geopolymer was influenced by the as-cured properties. The sintered kaolin-GGBS geopolymer also yielded the highest compressive strength. Direct sintering of the as-cured geopolymer transformed the main kaolinite phases into various phases. The adequate curing condition and two-steps of the sintering profile had reduced the risk of cracking commonly occurring in as-cured geopolymers.

Author Contributions: Conceptualization, N.H.J., M.M.A.B.A., B.J., and M.N.; data curation, I.H.A.A.; formal analysis, N.H.J., F.C.P., and M.H.; investigation, N.H.J., W.M.A.W.I., and I.H.A A.; methodology, N.H.J., M.M.A.B.A., F.C.P., M.H., B.J., and M.N.; project administration, F.C.P. and I.H.A.A.; software, N.H.J. and W.M.A.W.I.; visualization, W.M.A.W.I.; writing—original draft, N.H.J. and M.M.A.B.A. All authors have read and agreed to the published version of the manuscript.

Funding: This research was funded by the European Union—sponsoring the "Partnership for Research in Geopolymer Concrete" (PRI-GeoC-689857) grant.

Data Availability Statement: The data presented in this study are available in this article.

Acknowledgments: The authors gratefully acknowledge the Centre of Excellence for Geopolymers and Green Technology, (CeGeoGTech), UniMAP for the financial support. The authors would also like to extend their gratitude to the Faculty of Chemical Engineering Technology, Universiti Malaysia Perlis.

Conflicts of Interest: The authors declare no conflict of interest.

References

1. Heah, C.Y.; Kamarudin, H.; Mustafa Al Bakri, A.M.; Bnhussain, M.; Luqman, M.; Khairul Nizar, I.; Ruzaidi, C.M.; Liew, Y.M. Kaolin-based geopolymers with various NaOH concentrations. *Int. J. Miner. Metall. Mater.* **2013**, *20*, 313–322. [CrossRef]
2. Zhang, B.; Guo, H.; Deng, L.; Fan, W.; Yu, T.; Wang, Q. Undehydrated kaolinite as materials for the preparation of geopolymer through phosphoric acid-activation. *Appl. Clay Sci.* **2020**, *199*, 105887. [CrossRef]
3. Zhang, Z.H.; Zhu, H.J.; Zhou, C.H.; Wang, H. Applied Clay Science Geopolymer from kaolin in China: An overview. *Appl. Clay Sci.* **2016**, *119*, 31–41. [CrossRef]
4. Ganapathe, L.S.; Mohamed, M.A.; Mohamad Yunus, R.; Berhanuddin, D.D. Magnetite (Fe_3O_4) Nanoparticles in Biomedical Application: From Synthesis to Surface Functionalisation. *Magnetochemistry* **2020**, *6*, 68. [CrossRef]
5. Zannerni, G.M.; Fattah, K.P.; Al-Tamimi, A.K. Ambient-cured geopolymer concrete with single alkali activator. *Sustain. Mater. Technol.* **2020**, *23*. [CrossRef]
6. Zaribi, M.; Samet, B.; Baklouti, S. Effect of curing temperature on the synthesis, structure and mechanical properties of phosphate-based geopolymers. *J. Non Cryst. Solids* **2019**, *511*, 62–67. [CrossRef]
7. Jaya, N.A.; Al Bakri Abdullah, M.M.; Ghazali CM, R.; Hussain, M.; Hussin, K.; Ahmad, R. Kaolin Geopolymer as Precursor to Ceramic Formation. *MATEC Web Conf.* **2016**, *78*, 01061. [CrossRef]
8. Rincón, A.; Desideri, D.; Bernardo, E. Functional glass-ceramic foams from 'inorganic gel casting' and sintering of glass/slag mixtures. *J. Clean. Prod.* **2018**, *187*, 250–256. [CrossRef]
9. Ranjbar, N.; Kuenzel, C.; Spangenberg, J.; Mehrali, M. Hardening evolution of geopolymers from setting to equilibrium: A review. *Cem. Concr. Compos.* **2020**, *114*, 103729. [CrossRef]
10. Ranjbar, N.; Mehrali, M.; Alengaram, U.J.; Metselaar, H.S.C.; Jumaat, M.Z. Compressive strength and microstructural analysis of fly ash/palm oil fuel ash based geopolymer mortar under elevated temperatures. *Constr. Build. Mater.* **2014**, *65*, 114–121. [CrossRef]
11. Majhi, R.K.; Nayak, A.N. Bond, durability and microstructural characteristics of ground granulated blast furnace slag based recycled aggregate concrete. *Constr. Build. Mater.* **2019**, *212*, 578–595. [CrossRef]
12. Mierzwiński, D.; Łach, M.; Hebda, M.; Walter, J.; Szechyńska-Hebda, M.; Mikuła, J. Thermal phenomena of alkali-activated metakaolin studied with a negative temperature coefficient system. *J. Therm. Anal. Calorim.* **2019**, *138*, 4167–4175. [CrossRef]
13. Chen, C.Y.; Tuan, W.H. The processing of kaolin powder compact. *Ceram. Int.* **2001**, *27*, 795–800. [CrossRef]
14. Lao, X.; Xu, X.; Jiang, W.; Liang, J.; Miao, L.; Wu, Q. Influences of impurities and mineralogical structure of different kaolin minerals on thermal properties of cordierite ceramics for high-temperature thermal storage. *Appl. Clay Sci.* **2020**, *187*, 105485. [CrossRef]
15. Wei, W.; Yong, L.; Tan, Y.; Grover, L.; Guo, Y.; Bowei, L. A mica/nepheline glass-ceramic prepared by melting and powder metallurgy at low temperatures. *Mater. Today Commun.* **2017**, *11*, 87–93. [CrossRef]
16. Merabtene, M.; Kacimi, L.; Clastres, P. Elaboration of geopolymer binders from poor kaolin and dam sludge waste. *Heliyon* **2019**, *5*. [CrossRef]